Aptamer-conjugated optical nanomaterials for bioanalysis

Quan Yuan[a,c], Danqing Lu[a], Xiaobing Zhang[a], Zhuo Chen[a], Weihong Tan[a,b]

We review advances in the development and the application of optical biosensing systems based on aptamers. Aptamers exhibit advantages as molecular recognition elements for biosensors when compared to traditional antibodies. Among different detection modes that have been employed, optical methods are among the most used, and the combination of aptamers with novel optical nanomaterials has significantly improved the performance of aptamer-based sensors.

The review briefly introduces the unique optical properties of nanoscale materials and the urgency of research on aptamer-conjugated optical nanomaterials in bioanalysis. We then discuss current research activities with typical examples of fluorescence, surface-plasmon resonance and quencher nanomaterials for different detection methods (e.g., fluorescence resonance transfer, colorimetry, and surface-enhanced Raman scattering spectroscopy). The conclusion summarizes this exciting realm of study and offers perspectives for future developments.

Abbreviations: 4-ABT, 4-aminobenzenethiol; Apt-AuNP, Gold nanoparticle modified with an aptamer; AuNP, Gold nanoparticle; CNT, Carbon nanotube; CRET, Chemiluminescence resonance energy transfer; DMDAP, *N,N*-dimethyl-2,7-diazapyrenium; ds-DNA, Double stranded DNA; FRET, Fluorescence resonance-energy transfer; GO, Graphene oxide; GO-nS, Graphene oxide nanosheet; NIR, Near infrared; NP, Nanoparticle; PDGF, Platelet-derived growth factor; PDGFR, Platelet-derived growth factor receptor; QD, Quantum dot; rGO, Reduced graphene oxide; ROX, 6-carboxyl-X-rhodamine; SELEX, Systematic evolution of ligands by exponential enrichment; SERS, Surface-enhanced Raman scattering spectroscopy; SOG, Singlet-oxygen generation; SPR, Surface-plasmon resonance; ss-DNA, Single-stranded DNA; SWCNT, Single-walled CNT

Keywords: Aptamer; Bioanalysis; Biosensor; Colorimetry; Fluorescence; Nanomaterial; Optical sensing; Quencher; Surface-enhanced Raman scattering spectroscopy; Surface-plasmon resonance

Quan Yuan*, Danqing Lu, Xiaobing Zhang, Zhuo Chen, Weihong Tan*,
Molecular Science and Biomedicine Laboratory,
State Key Laboratory for Chemo/Biosensing and Chemometrics,
College of Biology, College of Chemistry and Chemical Engineering,
Hunan University,
Changsha 410082,
China

Weihong Tan*
Department of Chemistry and Shands Cancer Center,
Center for Research at Bio/nano Interface,
University of Florida, Gasinesville,
32611 FL,
USA

Quan Yuan*
Key Laboratory of Analytical Chemistry for Biology and Medicine
(Ministry of Education),
College of Chemistry and Molecular Sciences,
Wuhan University,
Wuhan 430072,
China

*Corresponding authors.
Tel.: +86 27 6875 6362;
Tel.: +1 352 846 2410;
E-mail:
yuanquanpku@gmail.com,
tan@chem.ufl.edu,

1. Introduction

The physical and chemical properties of matter are, to a large degree, determined by the type of motion its electrons are allowed to execute. The electronic motion, in turn, depends on the type of material and the space accessible to its electrons. The electronic structure is altered from continuous electronic bands to discrete or quantized electronic levels when the electrons are confined to the nanometer (nm) scale. As a result, continuous optical transitions between electronic bands become discrete, and new properties appear as the size of materials is decreased to the nm regime (in the 1–100 nm range). For example, noble-metal nanoparticles (NPs) have the ability to confine resonant photons within their small particle sizes to induce localized surface-plasmon oscillations of the conduction-band electrons [1–3]. This photon confinement increases the amplitude of the light wave by orders of magnitude, which dramatically increases

0165-9936/$ - see front matter © 2012 Elsevier Ltd. All rights reserved. doi:http://dx.doi.org/10.1016/j.trac.2012.05.010

Please cite this article in press as: Q. Yuan et al., Trends Anal. Chem. (2012), http://dx.doi.org/10.1016/j.trac.2012.05.010

the light intensity, which is proportional to the square of the wave's amplitude. In this manner, noble-metal NPs, through plasmonic confinement, effectively focus resonantly coupled light. As a result, all the optical properties of metal NPs (e.g., light absorption, fluorescence, Rayleigh scattering, and Raman scattering) are enhanced by orders of magnitude [4]. Other examples include quantum dots (QDs), whose sizes reach the 2–10 nm range, which are often comparable to or smaller than their exciton Bohr radii. The motion of their charge carriers becomes confined (quantum confinement), leading to unique absorption and fluorescence properties that depend on both particle size and particle shape [5,6].

Their small size, large surface area-to-volume ratio, and unique optical properties make optical nanomaterials excellent platforms for signal-reporter elements in constructing new optical sensors for bioanalysis. Both enhanced biocompatibility and biofunctionality can be achieved by surface modification with biomolecules. In particular, aptamers, which have highly specific molecular recognition properties, have played an important role in bioanalysis by conjugating with these optical nanomaterials.

Aptamers, first reported by three groups independently in 1990 [7–9], are single-stranded oligonucleotides generated *in vitro* by a process known as systematic evolution of ligands by exponential enrichment (SELEX). By folding into distinct secondary or tertiary structures, aptamers can specifically bind to certain targets with extremely high specificity. Due to the highly specific affnity of an aptamer to its target species {metal ions [10], small molecules, [11] proteins [12], whole cells [13,14], and even tissues [15]}, aptamers are considered to be chemical antibodies, with dissociation constants ranging from nanomolar to picomolar levels (nM–pM). Indeed, as a relatively new class of affinity agents, aptamers have the potential to achieve the same utility as antibodies. However, compared to antibodies, aptamers present a number of unique features that make them more effective choices:

(1) aptamers can be screened via an *in vitro* process against a synthetic library, making selection possible for any given target (from small metal ions to entire cells);
(2) aptamers are much more stable than antibodies and can undergo subsequent amplification through the polymerase chain reaction to produce a large quantity with high purity and lower cost than antibodies;
(3) the simple chemical structures of aptamers allow for further modification with functional groups to achieve specific purposes; and, finally,
(4) in addition to the specific molecular targeting, aptamers are capable of recognition through base-pairing, enabling tailorable designs for different bioanalysis applications.

Due to these advantages, the construction of aptamer-based bioconjugates results in structures capable of precise molecular recognition and enhanced target specificity according to pre-defined biochemical and biomedical applications. The two essential characteristics of biosensors are molecular recognition and signal transduction. In a conjugated system comprising an aptamer and an optical nanomaterial, the aptamer recognizes the target, and the optical nanomaterial provides signal transduction and signal amplification. Thus, the integration of aptamers and optical nanomaterials will lead to promising constructs for biosensing platforms.

In recent years, several reviews of aptamers appeared with various emphases [16–20]. In this article, we attempt to cover major advances in bioanalytical applications of aptamer-conjugated optical nanomaterials in recent years. To demonstrate this point, various detection techniques, including fluorescence, surface-plasmon resonance (SPR), surface-enhanced Raman scattering (SERS), and fluorescence resonance-energy transfer (FRET), are examined using typical examples. We discuss the integration of aptamers with different optical nanomaterials {e.g., QDs, metal NPs, carbon nanotubes (CNTs), graphene oxide (GO), and silica NPs (SiNPs)}. Finally, we provide some prospects for the near future.

2. Fluorescent nanomaterials

Because aptamers can be easily modified with a variety of organic dyes, fluorophore-based detection methods have been the most widely demonstrated [21]. Compared to organic fluorophores and dyes, which are the most commonly used bio-labeling reagents, QDs have a number of attractive optical properties, including greater photostability, high quantum yields, size-tunable photoluminescence spectra, and continuous absorption spectra covering the ultraviolet (UV) to near-infrared (NIR) ranges [22,23]. Furthermore, QDs are far more resistant to photobleaching than conventional organic fluorophores. Because of these superior photophysical properties, a great deal of attention has been focused on imaging applications of QDs [24–26]. Researchers are now recognizing that QDs can be more than passive labels and stains for bioanalysis.

The first example of aptamer-conjugated QDs was reported by Ellington for fluorescent detection of thrombin [27]. In this work, thrombin aptamers conjugated to QDs were hybridized with a complementary DNA strand labeled with a quencher at the end. Hybridization brought the QDs and ends into close proximity, resulting in fluorescence quenching by means of energy transfer from the QDs to the quencher. However, the presence of thrombin recovered the fluorescence signal, since the thrombin-aptamer interaction induced the release of the complementary quencher-labeled strand.

Please cite this article in press as: Q. Yuan et al., Trends Anal. Chem. (2012), http://dx.doi.org/10.1016/j.trac.2012.05.010

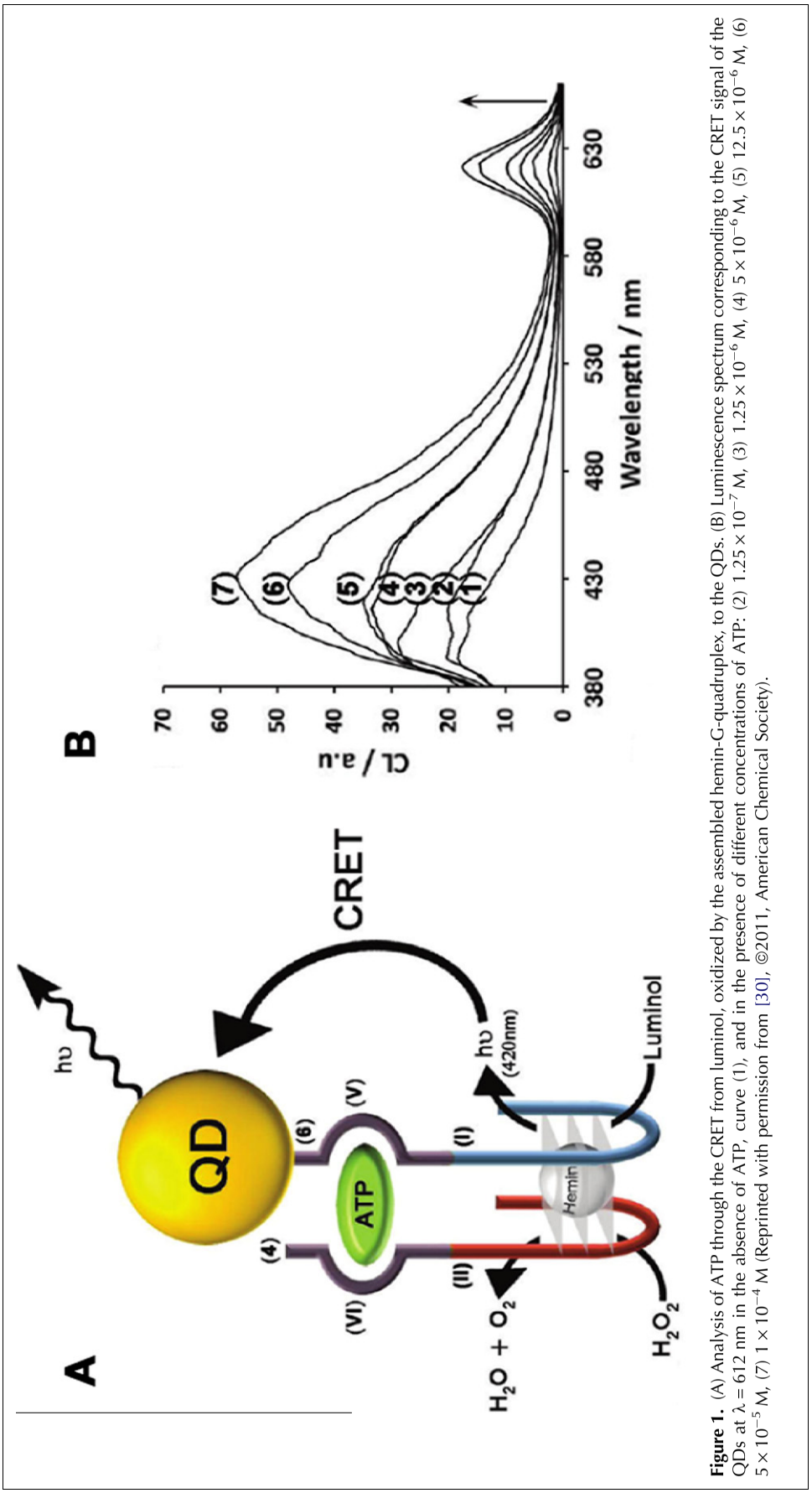

Figure 1. (A) Analysis of ATP through the CRET from luminol, oxidized by the assembled hemin-G-quadruplex, to the QDs. (B) Luminescence spectrum corresponding to the CRET signal of the QDs at $\lambda = 612$ nm in the absence of ATP, curve (1), and in the presence of different concentrations of ATP: (2) 1.25×10^{-7} M, (3) 1.25×10^{-6} M, (4) 5×10^{-6} M, (5) 12.5×10^{-6} M, (6) 5×10^{-5} M, (7) 1×10^{-4} M (Reprinted with permission from [30], ©2011, American Chemical Society).

Please cite this article in press as: Q. Yuan et al., Trends Anal. Chem. (2012), http://dx.doi.org/10.1016/j.trac.2012.05.010

Due to their broad absorption ranges, QDs with multiplex emissions can be simultaneously excited by a single wavelength light source [28]. Aptamer-conjugated QDs with different emissions have been successfully applied to detect cocaine and adenosine simultaneously [29].

Recently, Willner reported the novel photophysical phenomenon – that the G-quadruplex/hemin structure conjugated to semiconductor QDs can promote chemiluminescence resonance-energy transfer (CRET) to semiconductors [30]. In their design, nucleic-acid subunits consisted of fragments of horseradish peroxidase (HRP)-mimicking DNAzyme and aptamer domains against ATP (Fig. 1). In the presence of ATP, self-assembly into the active hemin-G-quadruplex DNAzyme structure resulted in CRET to Cd/ZnS QDs. The DNAzyme-generated CRET signal provided the optical read-out for the sensing event, resulting in a new aptamer-substrate-complex detection platform. Since many aptamer sequences form G-quadruplexes, the incorporation of the hemin into such G-quadruplexes might lead to chemiluminescence labels, provided that the resulting hemin/G-quadruplexes are catalytically active.

Based on this design, Willner recently reported that the incorporation of hemin into the aptameric G-quadruplex-thrombin complex led to a catalytic chemiluminescent DNAzyme structure that generated chemiluminescence in the presence of H_2O_2/luminol [31]. The conjugation of the nanostructures to CdSe/ZnS QDs yielded new CRET-based aptasensors for thrombin and ATP. Significant advantages accrue from application of the CRET process as a read-out signal:

(1) the close proximity between the chemiluminescent probe and the QDs eliminates background signals (e.g., of diffusional hemin); and,
(2) the possibility to excite different-sized QDs with the chemiluminescence signal enables the generation of different luminescence spectra controlled by the different QDs, thus allowing the construction of multiplexed aptamer-based sensors.

However, several properties limit the widespread use of QDs:

(1) they are composed of toxic heavy metals (e.g., cadmium), so cytotoxicity is a definite concern for *in vivo* applications;
(2) they are not soluble in water, and must be surface modified with a polymer to allow for use in biological applications; and,
(3) single colloidal QDs emit intermittently (so-called ''blinking'' behavior), which is a limiting factor for single-particle tracking within cells.

Recently, dye-doped SiNPs have emerged as particularly interesting fluorescent probes and have attracted widespread interest in biology and medicine [32–34]. The variety of chemical modifications of silica increases its versatility, and its biocompatibility makes it a relatively benign material. SiNPs are highly hydrophilic and easy to centrifuge for separation, surface modification and labeling procedures. Compared to organic fluorophores, which are the most commonly used bio-labeling reagents, fluorescent SiNPs can trap hundreds of fluorophores with large fluorescent signal amplification. Furthermore, they demonstrate the advantages of multiplexing capabilities, ease of functionalization, greater sensitivity and photostability. The advanced optical features of fluorescent SiNP probes are critical for ultrasensitive detection, real-time tracking and monitoring of complex biological events at the cellular level, which cannot be accomplished using regular fluorescent dyes. Conjugated with aptamers, dye-doped SiNPs have been developed as excellent labeling reagents for the detection of small molecules [35,36] and proteins [37].

As a consequence of aptamers' high binding affinity and excellent binding specificity, aptamer-conjugated dye-doped SiNPs have been increasingly used in early diagnostics. Sensitive detection of CEM cells has been achieved using sgc8 aptamer conjugated to dye-doped SiNPs [38].

The Tan group designed dye-doped SiNPs that used FRET as the emission scheme [39]. Three different organic dyes, FITC, R6G, and 6-carboxyl-X-rhodamine (ROX), which have overlapping emission and excitation spectra, are incorporated into the same silica matrix. By doping with different combinations of the three dyes, barcode tags can be produced for multiplexed, targeted FRET under single-wavelength excitation. Based on this successful synthesis, multiplexed cancer-cell detection was achieved by conjugating this triad of dye-doped SiNPs with three different aptamers specific for three individual cancer cell types (Fig. 2) [40]. FAM-doped SiNPs were conjugated with T1 aptamer for Toledo cells; FAM-doped and R6G-doped SiNPs were conjugated with sgc8 aptamer for CEM cells; and FAM-doped, R6G-doped, and ROX-doped SiNPs were conjugated with td05 aptamer for Ramos cells. Both flow-cytometry histograms and confocal-microscopy images showed the selectivity of this assay. Because of the FRET phenomenon between FAM, R6G and ROX dyes, different emissions were produced using a single excitation. When compared to single dye-doped SiNPs, these QD-like, multiple-dye-doped SiNPs greatly simplified the instrumental set-up for multiplexed bioanalysis, since only one laser source was needed.

It was recently reported that carbon nanomaterials (e.g., CNTs and grapheme) also have fluorescence properties in the NIR range [41–44], arising from recombination of electron–hole pairs in localized electronic states, rather than from band-edge transitions, as is the case in typical semiconductors. This property renders CNTs excellent candidates for biological optical probes, since spectral information is transferred efficiently in the range of the so-called tissue-transparent

Please cite this article in press as: Q. Yuan et al., Trends Anal. Chem. (2012), http://dx.doi.org/10.1016/j.trac.2012.05.010

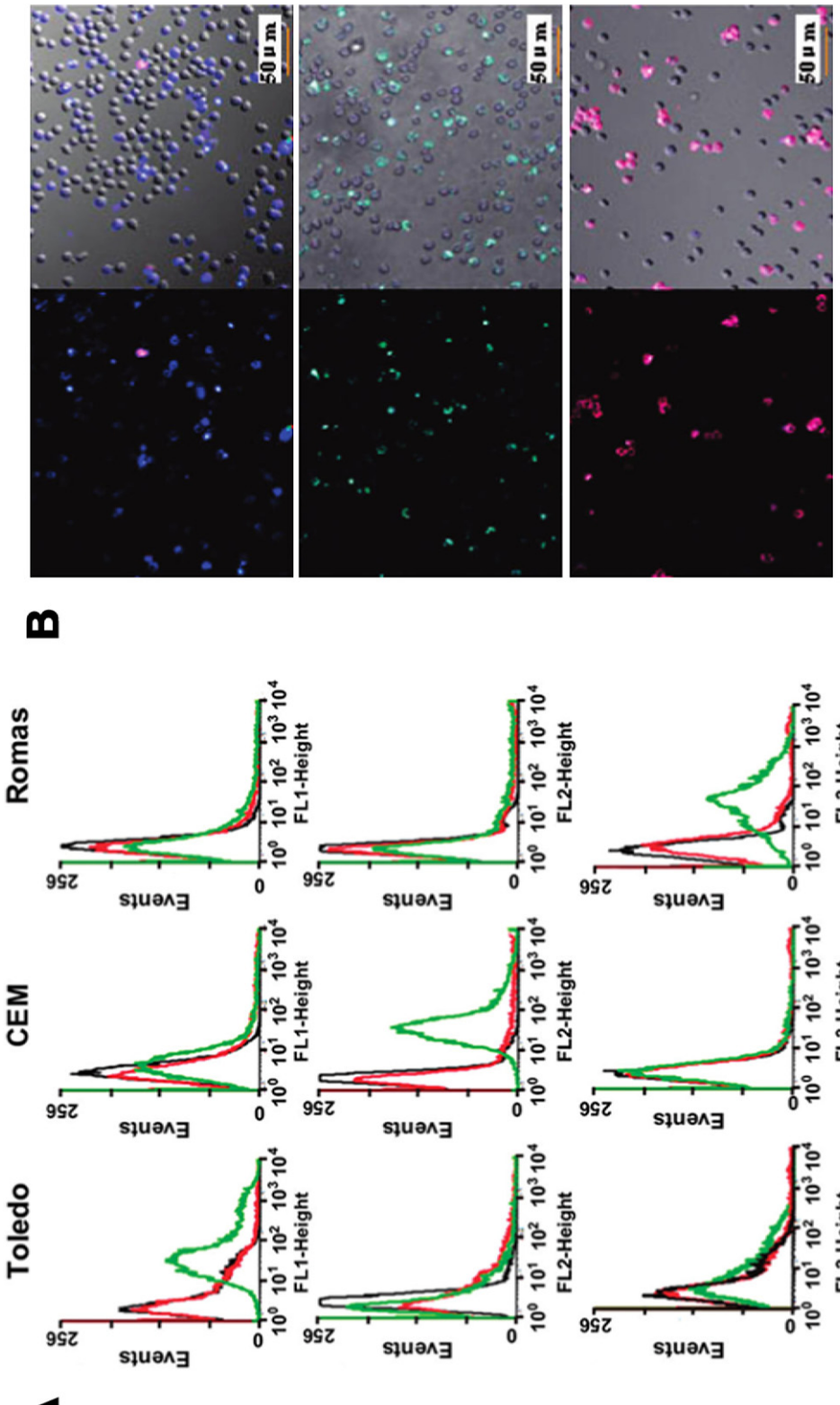

Figure 2. (A) Flow-cytometry histograms of aptamer-conjugated dye-doped silica nanoparticles (NPs) with three different cells: Top row, T1 aptamer conjugated to FAM-doped particles; middle row, sgc8 aptamer conjugated to FAM- and R6G-doped particles; bottom row, td05 aptamer conjugated to FAM-, R6G- and ROX-doped particles. On each histogram, the black curve corresponds to cells only; the red curve corresponds to dye-doped silica NPs (SiNPs) with cells; and, the green curve corresponds to aptamer-conjugated dye-doped SiNPs with cells. (B) Confocal microscopy images of aptamer-conjugated dye-doped SiNPs with a mixture of three different cells: Top row, T1 aptamer conjugated to FAM-doped particles; middle row, sgc8 aptamer conjugated to FAM- and R6G-doped particles; bottom row, td05 aptamer conjugated to R6G- and ROX-doped particles (Reprinted with permission from [40], ©2009, American Chemical Society).

Please cite this article in press as: Q. Yuan et al., Trends Anal. Chem. (2012), http://dx.doi.org/10.1016/j.trac.2012.05.010

window, where absorption and autofluorescence by biological substances are minimal [45,46]. Photoluminescence (PL) of CNT is also very sensitive to molecular binding events at the tube sidewall [47–49]. Also, the graphitic lattice allows non-covalent conjugation with biomolecular recognition elements (e.g., DNA oligonucleotides), which preserve CNTs' pristine electronic structures and thus their distinct optical signatures in aqueous solution [50,51].

An optical nanosensor architecture based on aptamer-conjugated NIR fluorescent single-walled CNTs (SWCNTs) was designed to detect cell-signaling molecules non-invasively in real time [52]. This sensor platform includes SWCNTs functionalized with insulin-binding aptamer to modulate NIR emission upon recognizing signaling molecules secreted from live cells cultured on an extracellular matrix in response to stimuli (Fig. 3). A 30-nt aptamer, which retained a four-stranded, parallel G quadruplex conformation on SWCNTs, was used to recognize insulin analytes selectively. A photoinduced charge-transfer mechanism led to highly selective photoluminescence quenching upon analyte binding with a limit of detection (LOD) of ~10 nM for insulin. The biosensor architecture developed in this study may be applied to other analytes of interest by incorporating appropriate aptamer sequences and could improve detection sensitivity to the single-analyte-molecule level if individual CNTs are examined [53].

3. Plasmonic nanomaterials

Plasmonics is a thriving new field that studies the electromagnetic responses of metal nanostructures to interactions with light at the metal-dielectric interface [54]. When resonant photons are confined within a plasmonic NP, they excite localized surface-plasmon oscillations, which give rise to strong surface electromagnetic fields that propagate around the particle and decay exponentially over a distance comparable to the particle size [55]. A red-shift of the surface-plasmon resonance (SPR) band occurs due to field coupling when plasmonic NPs come close together in a bulk solution, and this color change can be used for colorimetric detection [56]. This plasmonic near-field can also affect the properties of species in proximity to the metal NPs. For example, Raman scattering is enhanced for species adsorbed onto the surface of the particles [surface-enhanced Raman spectroscopy (SERS)] [57,58]. In fact, metal nanostructures can serve as fluorescence-signal intensifiers in different detection schemes [59,60]. Plasmonics has attracted

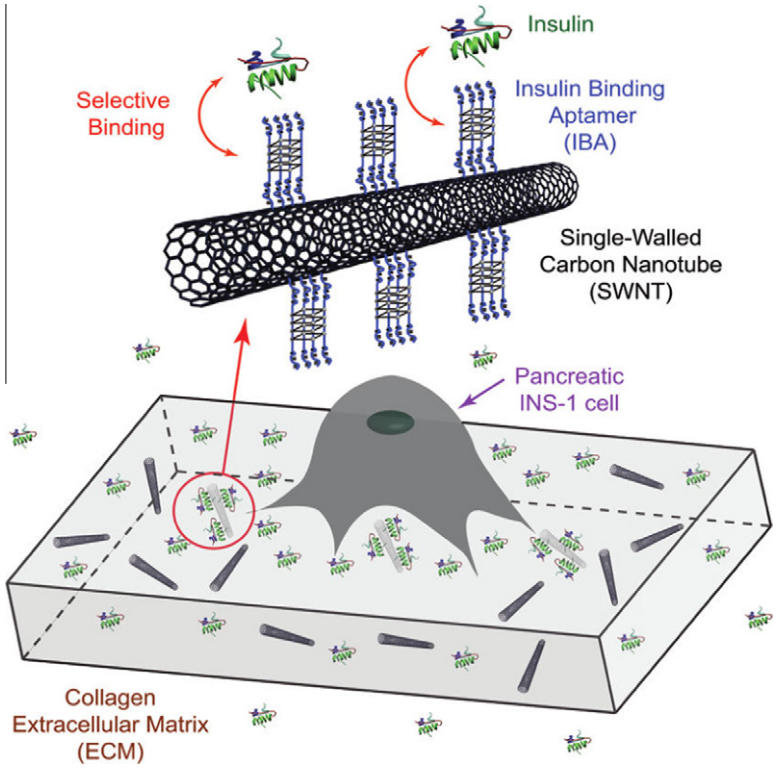

Figure 3. Optical nanosensor architecture for real-time measurement of insulin secreted from pancreatic INS-1 cells *in situ*. Near-IR fluorescent single-walled carbon nanotubes are non-covalently functionalized with insulin-binding aptamer to recognize target insulin and optically report with high selectivity and sensitivity (Reprinted with permission from [52], ©2011, American Chemical Society).

Please cite this article in press as: Q. Yuan et al., Trends Anal. Chem. (2012), http://dx.doi.org/10.1016/j.trac.2012.05.010

considerable interest due to its growing importance in the development of photonic, optoelectronic, and electronic devices (e.g., light-emitting diodes, lasers, superlenses, electronic circuits, and other applications) [61]. The high sensitivity of plasmon spectra to the particle size and local dielectric environment also provides a new methodology for detecting biomolecules, where the detection signal is solely based on changes in the plasmonic spectra [62,63].

Due to the surface-plasmon-band shift, the color of colloidal gold is sensitive to its aggregation (red to purple/blue) or dispersion (purple to red). Furthermore, because extinction coefficient of gold NPs (AuNPs) is over 1000 times higher than that of organic dyes [64], AuNP-based colorimetric detection provides considerable sensitivity. Assembly/disassembly of AuNPs can be considered as a novel indicator for colorimetric assays.

Chang et al. developed a highly specific sensing system for platelet-derived growth factors (PDGFs) and platelet-derived growth factor receptors (PDGFRs) by AuNPs modified with an aptamer (Apt-AuNPs) specific to PDGFs. PDGFs were detected by monitoring the changes in color and extinction of Apt-AuNPs that occurred as a result of aggregation [65].

Lu demonstrated a general design of colorimetric sensors based on the disassembly of NP aggregates linked by aptamers [66,67]. This kind of sensor was used to detect adenosine and cocaine. As no special features on the aptamers are required, the design should be applicable to any aptamer of choice. Inspired by the observation of Li and Rothberg that AuNPs preferably bind to single-stranded (ss-)DNA rather than to double-stranded (ds-)DNA [68,69], Fan reported a different approach using unmodified AuNPs to discriminate effectively target-bound, structured aptamers from unbound, random coil-like DNA [70]. They designed a novel aptamer-target-binding read-out strategy that translates an aptamer-target binding event to a duplex-to-aptamer dehybridization process, which can be conveniently detected with unmodified AuNPs in a colorimetric approach. The target-free aptamer was first hybridized with its complementary sequence, forming a rigid duplex (Fig. 4). In the presence of the specific target, the aptamer binds to the target and forms a structured complex, which disassembles the original duplex and releases an ssDNA strand. Then, unmodified AuNPs are used to interrogate this target-induced displacement process colorimetrically. This novel assay method is simple in design, avoiding oligonucleotide labeling and AuNP modification.

Instead of simple aggregation of the AuNPs using DNA or proteins, a direct colorimetric assay for cancer cells has been developed in the Tan group by assembly of AuNPs on cell-membrane surfaces *via* the recognition between aptamers and their target proteins on the cell membrane [71]. This, in turn, causes the SPR bands of the AuNPs to overlap, providing a direct visualization of CEM cells by using sgc8-conjugated AuNPs and Ramos cells by tdo5-conjugated AuNPs.

Adapting a similar design, Zeng et al. fabricated a strip biosensor for sensitive detection of circulating tumor cells, using Ramos cells as proof of principle [72]. The presence of 4000 Ramos cells was detectable by the naked eye, and as few as 800 Ramos cells could be detected by a portable strip reader.

Theoretical [73] and experimental [74,75] results have proved that an enhanced Raman scattering signal could presumably emanate from the large

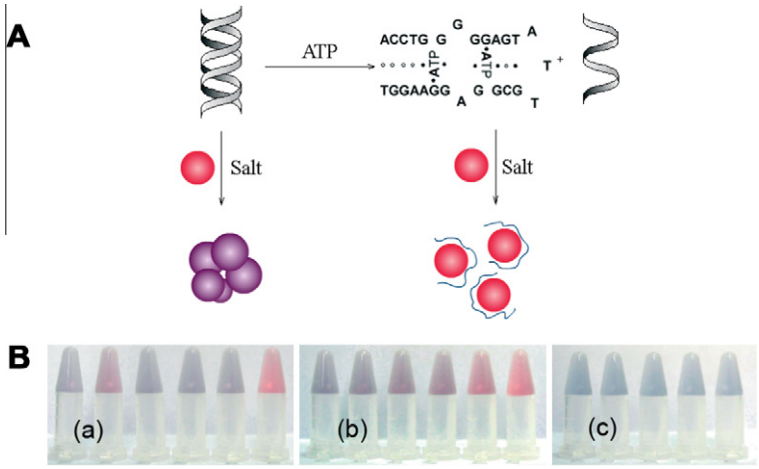

Figure 4. (A) AuNP-based aptamer-target binding readout strategy for ATP assay. (B) (a) Unmodified AuNPs selectively detect ATP. From left to right: dsDNA; the duplex system incubated with 22.1 μM ATP, CTP, UTP and GTP; and, only ssDNA; (b) Colorimetric detection of ATP with various concentrations. From left to right: 0, 1.1, 8.9, 22.1, 88.5, 132.7 μM ATP; (c) Control experiment showing that ATP alone (without the anti-ATP aptamer) does not affect the color of AuNPs. From left to right: 1.1, 8.9, 22.1, 88.5, 132.7 μM ATP (Reprinted with permission from [70] ©2007, Wiley-VCH Verlag GmbH & Co. KGaA).

Please cite this article in press as: Q. Yuan et al., Trends Anal. Chem. (2012), http://dx.doi.org/10.1016/j.trac.2012.05.010

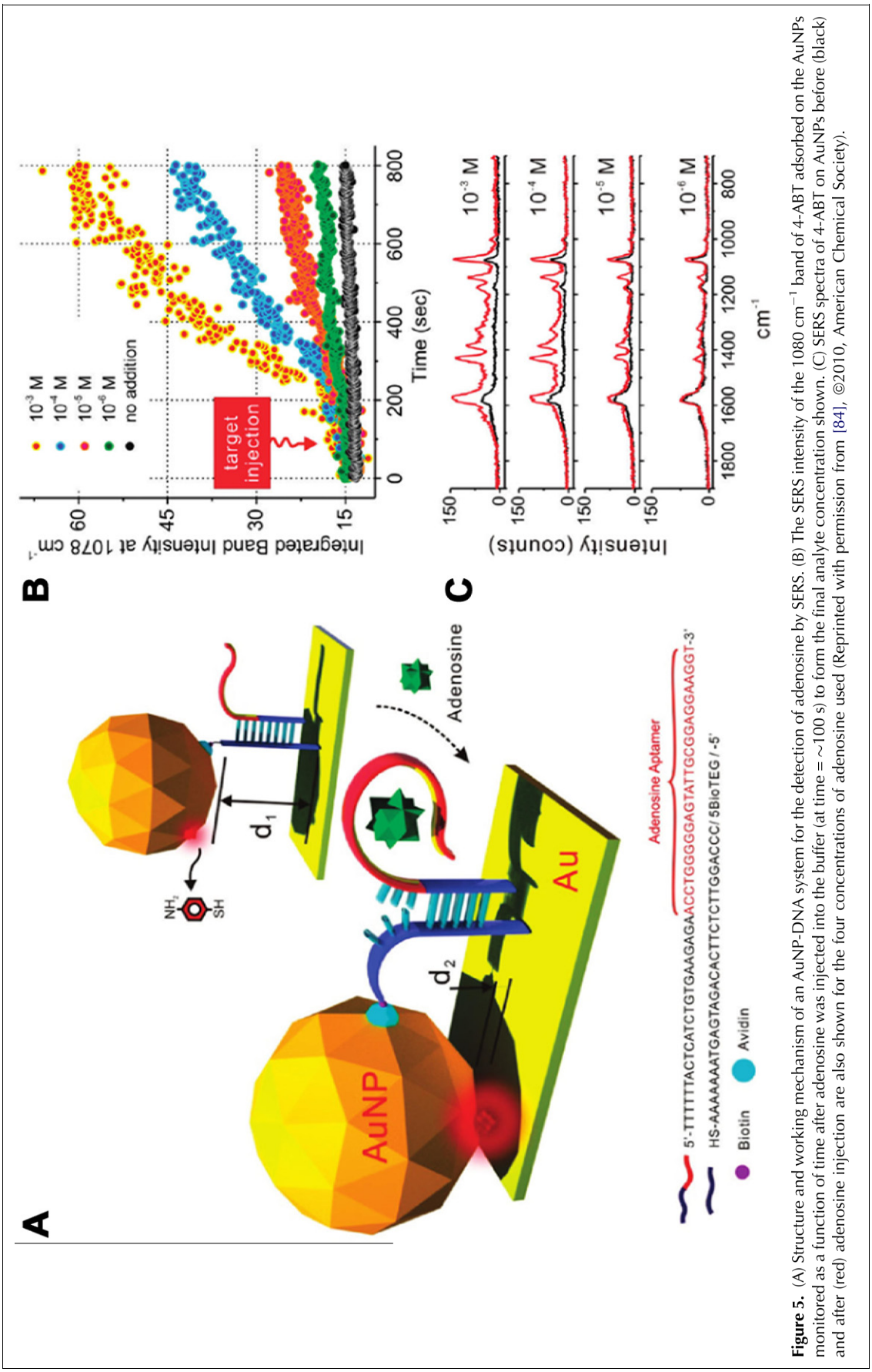

Figure 5. (A) Structure and working mechanism of an AuNP-DNA system for the detection of adenosine by SERS. (B) The SERS intensity of the 1080 cm^{-1} band of 4-ABT adsorbed on the AuNPs monitored as a function of time after adenosine was injected into the buffer (at time = ~100 s) to form the final analyte concentration shown. (C) SERS spectra of 4-ABT on AuNPs before (black) and after (red) adenosine injection are also shown for the four concentrations of adenosine used (Reprinted with permission from [84], ©2010, American Chemical Society).

Please cite this article in press as: Q. Yuan et al., Trends Anal. Chem. (2012), http://dx.doi.org/10.1016/j.trac.2012.05.010

electromagnetic field produced by SPR on metal nanostructures, particularly in "hot spots" at the gaps or junctions of an ensemble of structures [76,77]. Since the first discovery of SERS, it has been shown that the Raman scattering cross-section of a molecule can be increased up to 10^7–10^8 fold, making it a viable alternative to fluorescence sensors, so fabrication of junctions based on electromagnetic field hot spots by SERS could result in devices with high sensitivity and specificity for *in vitro* and *in vivo* biosensing [78–80].

Irudayaraj et al. fabricated a novel SERS aptasensor based on gold nanorod (AuNR)/AuNP composites for detection of thrombin in human-blood serum [81]. AuNRs were modified by thrombin-binding antibody to capture the target α-thrombin. AuNPs were conjugated with a corresponding Raman reporter-labeled aptamer to create a protein sandwich between the AuNRs and AuNPs for SERS detection. The interaction between α-thrombin and antibody brought AuNPs and AuNRs into close proximity to form a junction, giving rise to hot spots under laser excitation to produce an enhanced Raman scattering signal. In the absence of thrombin, the signal from AuNPs not bound to AuNRs did not contribute to any enhancement because of the size effect [82]. Dluhy described a highly-sensitive SERS-based method for detection of influenza viral nucleoproteins by AgNR arrays [83]. The intrinsic SERS spectrum of the aptamer–nucleoprotein complex provided direct evidence of binding between a polyvalent anti-influenza aptamer and the nucleoproteins of three influenza strains.

Moskovits et al. reported a SERS-based ''nose'', using a bifunctional adenosine-sensitive aptamer as an example. A SERS hot spot was created between a vapor-deposited bulk Au surface and an AuNP attached to the aptamer via a biotin-avidin linkage [84]. As shown in Fig. 5, the AuNP was decorated with the Raman tag molecule 4-aminobenzenethiol (4-ABT). When target molecule adenosine was added to the system in buffer, the SERS spectrum of 4-ABT increased in intensity by factors in the range ~1.3-~4, depending on the concentration of the analyte. *In situ* AFM imaging also confirmed the fact that the mean height of the AuNP-bearing aptamer decreased by ~5.6 nm, consistent with the observed SERS intensity change. This strategy may be further developed by using several bifunctional aptamers, each with its own Raman tag for simultaneous detection.

4. Quencher nanomaterials

FRET is a dipolar coupling interaction through space and it allows electronic energy to be transferred from a donor to an acceptor. The rate of energy transfer depends on the distance between the donor and the acceptor, their relative orientations, and the spectral overlap. The mathematical formula for FRET can be found in many reviews and book chapters [85–87]. In the derivation of the FRET formula, it is assumed that the donor and the acceptor can be represented as point dipoles. Fluorescent nanomaterials as donors for detection are described above. In this section, we present nanomaterials having quenching effects and acting as acceptors.

Although CNTs are themselves fluorescent, they can also quench fluorescence. These seemingly contradictory properties are a manifestation of the heterogeneous chemical, atomic and electronic structures of CNTs. The common absorption spectrum of a typical SWCNT sample spans a wide range of wavelengths from ~500–900 nm [88], significantly overlapping the photoluminescence spectra of various fluorophores. This allows resonant energy transfer (i.e. FRET) to occur from a photoexcited donor fluorophore to a ground-state acceptor SWCNT in the proximity of the donor [89]. SWCNTs have been demonstrated to be superior, universal quenchers for a variety of organic fluorophores. By employing DNA as the recognition component and a fluorophore as the label, the strong interaction between ssDNA and SWCNTs can bring the dye and SWCNTs into close proximity, thereby resulting in complete quenching. However, hybridization of the ssDNA to its complementary strand weakens the interaction with the SWCNT, and can even result in dissociation from the SWCNT. A sensing platform can be generated based on the different binding interactions between SWCNTs and ssDNA/dsDNA.

The Tan group has designed an effective fluorescent sensing platform based on the non-covalent assembly of SWCNTs and the dye-labeled aptamer of human α-thrombin [90]. In the absence of thrombin, the aptamer bonded non-covalently to the SWCNT *via* π-stacking between the nucleotide bases and the SWCNT side walls. Formation of the aptamer/SWCNT structure resulted in fluorescence quenching of the dye. When thrombin was added, the interaction of aptamer-SWCNTs with thrombin induced a conformational change in the aptamer, resulting in restoration of fluorescence.

A novel photosensitizer-aptamer-SWCNT complex was engineered to regulate singlet-oxygen generation (SOG) for photodynamic therapy [91]. Photosensitizer Ce6 was covalently attached to one end of the DNA aptamer. In the absence of target, Ce6-labeled aptamers wrapped onto the SWCNT surface, resulting in efficient quenching of SOG. However, upon target binding, the interaction between DNA and SWCNTs was disturbed to remove the aptamer from SWCNTs, leading to restoration of SOG.

In a similar manner, the sp^2 domains within GO and reduced GO (rGO) allow quenching of nearby fluorescent species {e.g., dyes [92,93], conjugated polymers [94,95] and QDs [96]}. The quenching efficiency of GO is significantly improved after reduction [93].

Please cite this article in press as: Q. Yuan et al., Trends Anal. Chem. (2012), http://dx.doi.org/10.1016/j.trac.2012.05.010

Fluorescence quenching has been used as the basis of GO optical sensors for sensing biomolecules [96–98]. The sensor concept is based on the fluorescence quenching of the dye-labeled ssDNA on binding with GO.

Yang et al. first reported a detection platform based on an aptamer/GO composite. Because of the strong binding affinity between GO and FAM-labeled thrombin aptamer, the quenching effect reached an efficiency of 96%. A significant fluorescence enhancement was observed after target-molecule thrombin was introduced [97].

Li and co-workers designed an aptamer/GO nanosheet (GO-nS) nanocomplex for *in situ* molecular probing in living cells [99], using ATP-ATP aptamer recognition as a model system. ATP aptamer labeled with the fluorophore FAM was incubated with GO-nS to form aptamer-FAM/GO-nS (Fig. 6). Nearly 100% fluorescence quenching with very rapid kinetics was observed. Addition of target ATP released the aptamer from the surface of GO-nS, and extraordinary fluorescence recovery was observed. The successful delivery to molecular targets in living cells suggests that GO could be a good vehicle to transport genes into cells, protecting the loading gene from enzymatic cleavage and enabling *in situ* molecular probing.

Besides having SPR properties, AuNPs also exhibit superquenching of fluorescence through energy/charge-transfer processes. The quenching constants of dye-AuNP pairs are usually several orders of magnitude greater than those of dye-organic quencher pairs [100].

Chang constructed a PDGF assay using aptamer-modified AuNPs [101]. The fluorophore *N,N*-dimethyl-2,7-diazapyrenium dication (DMDAP) can be intercalated with PDGF aptamer, which has a unique triple-helix conformation. Aptamer-AuNP composites brought AuNPs close to DMDAP and thus quenched the fluorescence. The conformation of the aptamer changed when binding with PDGF and therefore prevented DMDAP intercalation, inducing the recovery of fluorescence. Subsequently, the same group demonstrated a competitive homogeneous photoluminescence quenching assay of PDGF using photoluminescent gold nanodots as donors and AuNPs as acceptors [102].

Mirkin built aptamer nanoflares, which can directly quantify intracellular analyte in a living cell [103]. Aptamer nanoflares comprise an AuNP core functionalized with a dense monolayer of nucleic-acid ATP aptamers hybridized with short complementary Cy5-labeled reporter strands (Fig. 7). When the nanoflares met ATP inside living cells, the interaction between ATP and the aptamers led to a conformational change of the aptamers, displacing the Cy5-labeled strand to recover the fluorescence signal. This type of nanoconjugate is a promising approach for the intracellular quantification of small molecules in living cells.

FRET technology is very convenient and can be applied routinely for single-molecule detection. However, the length scale for detection in FRET-based methods is limited by the nature of the dipole-dipole mechanism, which effectively constrains distances to <10 nm [104–106]. Since FRET physically originates from the weak electromagnetic coupling of two dipoles, the FRET limit can be circumvented by introducing additional dipoles and thus providing more coupling interactions. Chance, Prock, and Silbey described the energy transfer from a dipole to a metallic surface, called surface-energy transfer (SET), at a much slower decay rate than the dipole-dipole energy transfer in FRET [105,107,108]. This arrangement effectively breaks the detection barriers of FRET, thereby increasing the probability of energy transfer.

The Tan group proposed using aptamer-AuNP conjugates to construct the first practical SET ruler for measuring the distance between two binding sites on a membrane receptor in live cells [109]. By taking advantage of the fixed binding-site distance on a receptor PTK7 in the lipid bilayer of the CEM cell membrane with two binding sites on its extracellular domain, the distance from the dye molecule to the metal-particle surface could be manipulated to determine the distance between the two binding sites on a live cell membrane (Fig. 8). Two ligands, sgc8 aptamer and anti-PTK7 antibody, were employed to bring organic fluorophore Alexa Fluor 488 and AuNPs to the binding sites on the cell membrane. The AuNPs were functionalized with excess thiol-modified sgc8 aptamers,

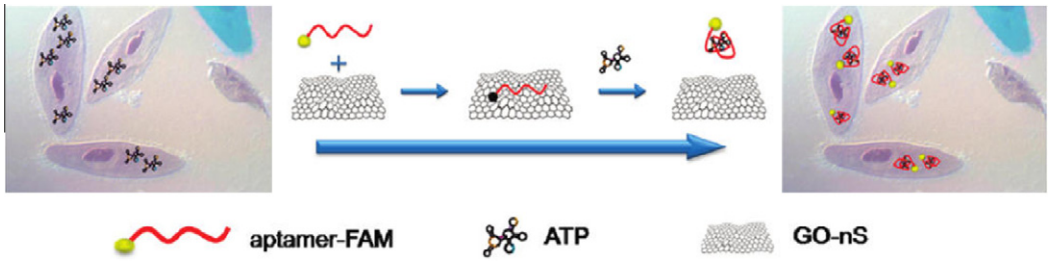

Figure 6. *In situ* molecular probing in living cells using an aptamer/GO-nS nanocomplex (Reprinted with permission from [99] ©2010, American Chemical Society).

Please cite this article in press as: Q. Yuan et al., Trends Anal. Chem. (2012), http://dx.doi.org/10.1016/j.trac.2012.05.010

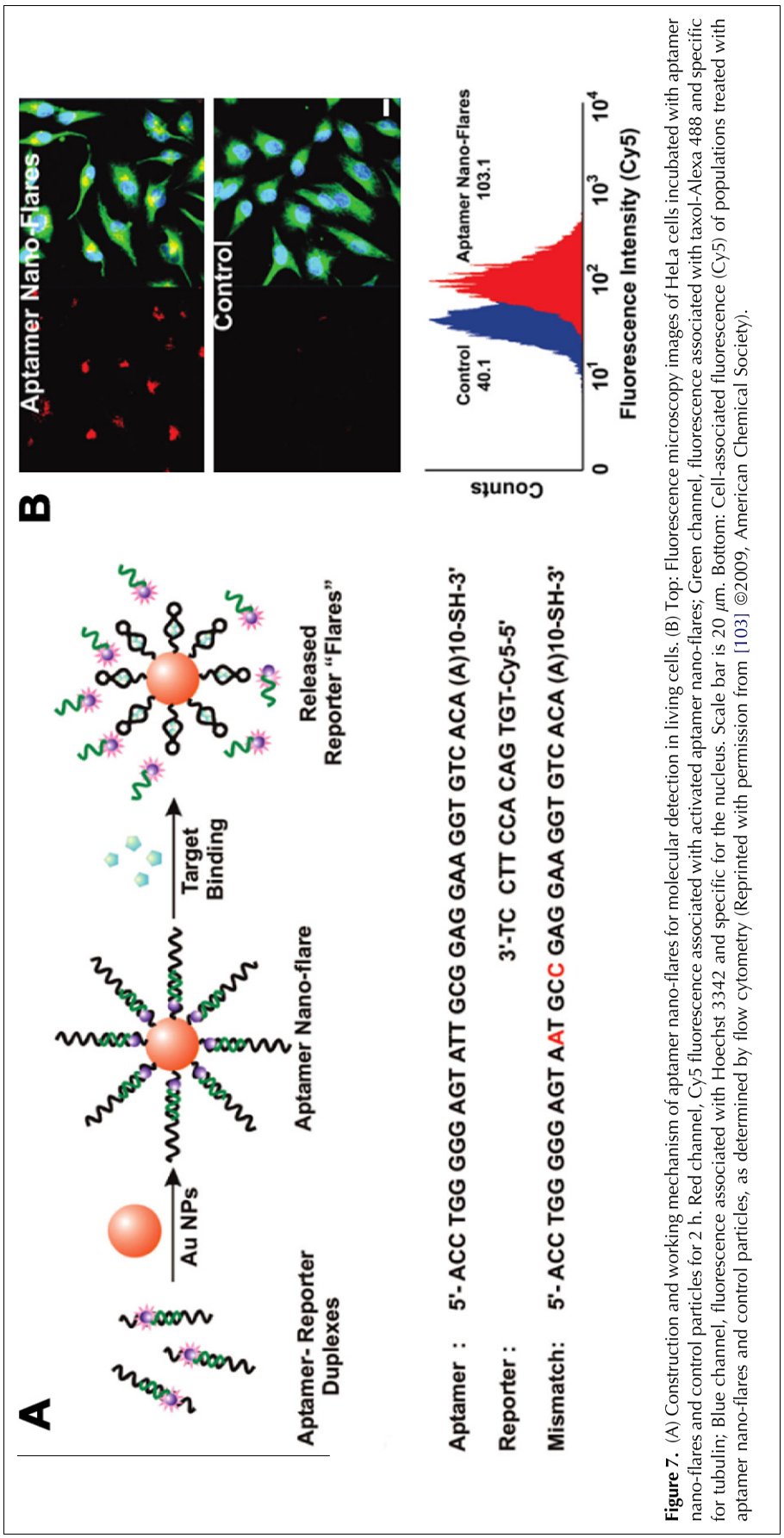

Figure 7. (A) Construction and working mechanism of aptamer nano-flares for molecular detection in living cells. (B) Top: Fluorescence microscopy images of HeLa cells incubated with aptamer nano-flares and control particles for 2 h. Red channel, Cy5 fluorescence associated with activated aptamer nano-flares; Green channel, fluorescence associated with taxol-Alexa 488 and specific for tubulin; Blue channel, fluorescence associated with Hoechst 3342 and specific for the nucleus. Scale bar is 20 μm. Bottom: Cell-associated fluorescence (Cy5) of populations treated with aptamer nano-flares and control particles, as determined by flow cytometry (Reprinted with permission from [103] ©2009, American Chemical Society).

Please cite this article in press as: Q. Yuan et al., Trends Anal. Chem. (2012), http://dx.doi.org/10.1016/j.trac.2012.05.010

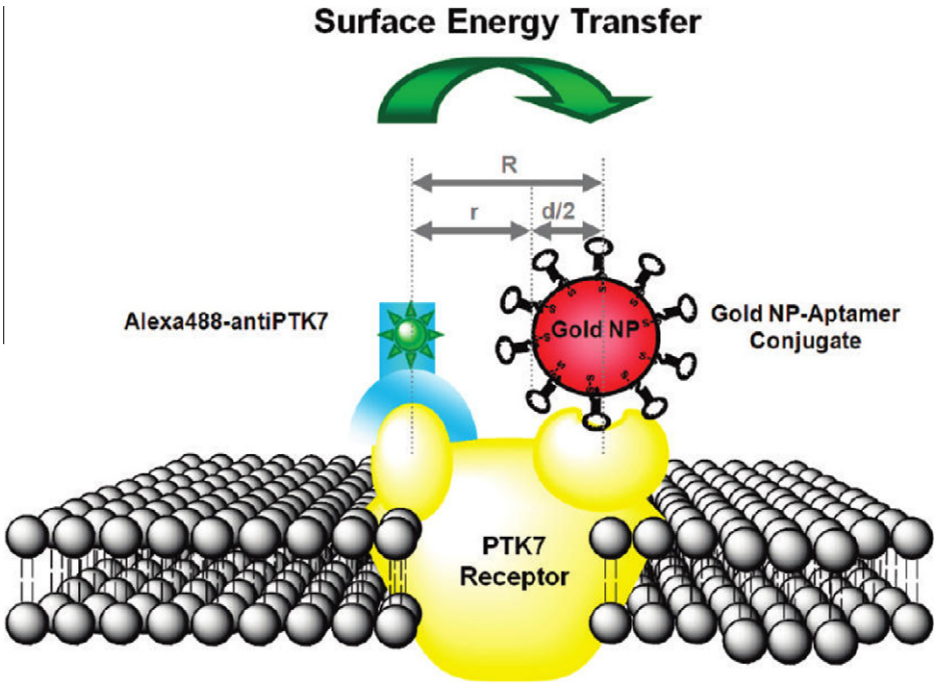

Figure 8. ''SET Nanoruler'' for measuring the distance between two binding sites in receptor PTK7 on a live cell membrane (Reprinted with permission from [109], ©2009, American Chemical Society).

and the antibody anti-PTK7 was modified with Alexa Fluor 488 through the primary amines on the heavy chain. As a consequence of the co-localization of the two binding sites on receptor PTK7, binding of ligands sgc8 and anti-PTK7 to their individual binding sites brought the Alexa Fluor 488 and AuNPs in close proximity for effective energy transfer. As shown in Fig. 8, the distance, R, from the fluorophore on the antibody binding site to the center of the NP on the aptamer is equivalent to the distance between the two binding sites on the PTK7 receptor. In addition, a series of AuNPs of different sizes were adopted to fit in the binding pockets to avoid steric effects. Therefore, by controlling the sizes of the AuNPs, the distance from the fluorophore molecule to the surface of AuNPs could be manipulated, and the relationship between the size of the AuNPs and the change in the energy-transfer efficiency could be evaluated.

5. Conclusion and trends

Nanomaterials with different optical properties provide powerful tools to design ideal signal-enhanced optical aptasensors. While aptasensors emerged only about 10 years ago, they have already found broad applications in bioanalysis. However, despite this attractive development, aptamer-based bioassays are still immature compared to immunoassays, due primarily to the limited availability of aptamer types and the relatively poor knowledge of surface-immobilization technologies for aptamers [16]. However, important advances have been realized in the past 10 years. For example, at this time, approximately 250 aptamers have been sequenced.

The recent progress in SELEX techniques enables rapid, efficient selection of aptamers for targets within only a few hours [110,111], compared to traditional SELEX requiring several weeks to months. As for detection methods, optical aptamer-based detection systems using new optical nanomaterials have enormous potential. The development of aptamer-conjugated optical nanomaterials for bioanalysis merges the fields of life science, materials science and chemistry. With the great progress in both aptamers and nanomaterials, these types of nanodevices show ideal performances for sensing.

As we have presented in this review, rapid advances in the design of new optical nanomaterials provides an opportunity for the development of optical nano-aptasensors. Materials scientists continue to explore new functional nanomaterials using a variety of synthetic methods. For example, non-linear optical nanomaterials (e.g., lanthanide-doped up-conversion NPs) have intense visible emissions under NIR excitation, which is less harmful to biological samples [112]. These have become more prominent in biological sciences, as the preparation of high-quality lanthanide-doped NPs has become increasingly routine [112,113]. However, few efforts have been devoted to develop aptasensors based on these kinds of materials [114].

Please cite this article in press as: Q. Yuan et al., Trends Anal. Chem. (2012), http://dx.doi.org/10.1016/j.trac.2012.05.010

The current state-of-the-art of aptamer-conjugated optical NPs has also been limited by the difficulty in bioconjugation chemistry. Various NPs prepared by conventional strategies have either no intrinsic aqueous solubility or lack functional organic moieties, so an additional surface-treatment step prior to bioconjugation is required. Although still a challenge for bioanalytical development, available chemistries are rapidly improving, allowing the advantages of nanomaterials to be maximized. Furthermore, most of the assays described above were demonstrated in buffer systems as proof-of-concept methods. For aptamer-conjugated optical nanomaterials to find practical applications in the analytical community, their performances need to be carefully evaluated for possible matrix effects in complex samples.

Another area of opportunity is the development of new optical detection techniques. Because fluorophores near a metallic surface have unique characteristics, including increased fluorescence intensity, quantum yield and photostability, recent research has focused on the near-field interaction between fluorophores and metals, especially the phenomenon of surface-plasmon-coupled directional emission, which can be used to develop new aptasensors [115,116]. Among the various devices that have been developed, the waveguide-mode device was also recently shown to be suitable for detecting target–aptamer interactions.

Optical microsphere resonators provide another new sensing mechanism for development of aptasensors. Unlike conventional waveguide-based biosensors, in which the light passes through the waveguide only once, the guided mode resonance circulates repeatedly around the spherical surface [117]. Optical resonances allow the light to interact with an analyte molecule several thousand times, thus lowering the LOD by several orders of magnitude, compared to single-pass techniques [118–120].

Acknowledgements

This work was supported by the National Natural Science Foundation of China (20975034), the National Key Scientific Program of China (2011CB911001, 2011CB911003), and China National Instrumentation Program 2011YQ03012412. This work was also supported by grants awarded by the National Institutes of Health (GM066137, GM079359 and CA133086).

Appendix A. Supplementary data

Supplementary data associated with this article can be found, in the online version, at http://dx.doi.org/10.1016/j.trac.2012.05.010.

References

[1] S.J. Oldenburg, R.D. Averitt, S.L. Westcott, N.J. Halas, Chem. Phys. Lett. 288 (1998) 243.
[2] H. Wang, D.W. Brandl, P. Nordlander, N.J. Halas, Acc. Chem. Res. 40 (2007) 53.
[3] P.K. Jain, X. Huang, I.H. El-Sayed, M.A. El-Sayed, Acc. Chem. Res. 41 (2008) 1578.
[4] M.D. Malinsky, K.L. Kelly, G.C. Schatz, R.P. Van Duyne, J. Am. Chem. Soc. 123 (2001) 1471.
[5] A.P. Alivisatos, J. Phys. Chem. 100 (1996) 13226.
[6] A.P. Alivisatos, Science (Washington, DC) 271 (1996) 933.
[7] C. Tuerk, L. Gold, Science (Washington, DC) 249 (1990) 505.
[8] A.D. Ellington, J.W. Szostak, Nature (London) 346 (1990) 818.
[9] D.L. Robertson, G.F. Joyce, Nature (London) 344 (1990) 467.
[10] H. Ueyama, M. Takagi, S. Takenaka, J. Am. Chem. Soc. 124 (2002) 14286.
[11] D.E. Huizenga, J.W. Szostak, Biochemistry 34 (1995) 656.
[12] L.C. Bock, L.C. Griffin, J.A. Latham, E.H. Vermaas, J.J. Toole, Nature (London) 355 (1992) 564.
[13] D. Shangguan, Y. Li, Z. Tang, Z.C. Cao, H.W. Chen, P. Mallikaratchy, K. Sefah, C.J. Yang, W. Tan, Proc. Natl. Acad. Sci. USA 103 (2006) 11838.
[14] X. Fang, W. Tan, Acc. Chem. Res. 43 (2010) 48.
[15] S. Li, H. Xu, H. Ding, Y. Huang, X. Cao, G. Yang, J. Li, Z. Xie, Y. Meng, X. Li, Q. Zhao, B. Shen, N. Shao, J. Pathol. 218 (2009) 327.
[16] S. Song, L. Wang, J. Li, J. Zhao, C. Fan, Trends Anal. Chem. 27 (2008) 108.
[17] A.D. Keefe, S. Pai, A. Ellington, Nat. Rev. Drug Discovery 9 (2010) 537.
[18] T. Chen, M.I. Shukoor, Y. Chen, Q. Yuan, Z. Zhu, Z. Zhao, B. Gulbakan, W. Tan, Nanoscale 3 (2011) 546.
[19] A.B. Iliuk, L. Hu, W.A. Tao, Anal. Chem. 83 (2011) 4440.
[20] R.M. Kong, X.B. Zhang, Z. Chen, W. Tan, Small 7 (2011) 2428.
[21] N.K. Navani, Y. Li, Curr. Opin. Chem. Biol. 10 (2006) 272.
[22] A.P. Alivisatos, A.L. Harris, N.J. Levinos, M.L. Steigerwald, L.E. Brus, J. Chem. Phys. 89 (1988) 3435.
[23] M. Nirmal, C.B. Murray, M.G. Bawendi, Phys. Rev. B 50 (1994) 2293.
[24] M. Bruchez, M. Morronne, P. Gin, S. Weiss, A.P. Alivisatos, Science (Washington, DC) 281 (1998) 2013.
[25] X. Gao, Y.Y. Cui, R.M. Levenson, L.W.K. Chung, S. Nie, Nature (London) 8 (2004) 969.
[26] X. Gao, L. Yang, J.A. Petros, F.F. Marshall, J.W. Simons, S. Nie, Curr Opin Biotechnol. 16 (2005) 63.
[27] M. Levy, S.F. Cater, A.D. Ellington ChemBioChem 6 (2005) 2163.
[28] W.C.W. Chan, D.J. Maxwell, X. Gao, R.E. Bailey, M. Han, S. Nie, Curr. Opin. Biotechnol. 13 (2002) 40.
[29] J. Liu, J.H. Lee, Y. Lu, Anal. Chem. 79 (2007) 4120.
[30] R. Freeman, X.Q. Liu, I. Willner, J. Am. Chem. Soc. 133 (2011) 11597.
[31] X. Liu, R. Freeman, E. Golub, I. Willner, ACS Nano 5 (2011) 7648.
[32] L. Wang, K.M. Wang, S. Swadeshmukul, X.J. Zhao, L.R. Hilliard, J. Smith, W. Tan, Anal. Chem. 78 (2006) 646A.
[33] G. Yao, L. Wang, Y. Wu, J. Smith, J. Xu, W. Zhao, E. Lee, W. Tan, Anal. Bioanal. Chem. 385 (2006) 518.
[34] H. Ow, D.R. Larson, M. Srivastava, B.A. Baird, W.W. Webb, U. Wiesner, Nano Lett. 5 (2005) 113.
[35] Y. Wang, Y. Wang, B. Liu, Nanotechnology 19 (2008) 415605.
[36] Y. Song, C. Zhao, J. Ren, X. Qu, Chem. Commun. (2009) 1975.
[37] X. Wang, J. Zhou, W. Yun, S. Xiao, Z. Chang, P. He, Y. Fang, Anal. Chim. Acta 598 (2007) 242.

Please cite this article in press as: Q. Yuan et al., Trends Anal. Chem. (2012), http://dx.doi.org/10.1016/j.trac.2012.05.010

[38] M.C. Estévez, M.B. O'Donoghue, X. Chen, W. Tan, Nano Res. 2 (2009) 448.
[39] L. Wang, W. Tan, Nano Lett. 6 (2006) 84.
[40] X. Chen, M.C. Estévez, Z. Zhu, Y.F. Huang, Y. Chen, L. Wang, W. Tan, Anal. Chem. 81 (2009) 7009.
[41] J.H. Choi, F.T. Nguyen, P.W. Barone, D.A. Heller, A.E. Moll, D. Patel, S.A. Boppart, M.S. Strano, Nano Lett. 7 (2007) 861.
[42] X. Sun, Z. Liu, K. Welsher, J.T. Robinson, A. Goodwin, S. Zaric, H. Dai, Nano Res. 1 (2008) 203.
[43] Z.T. Luo, P.M. Vora, E.J. Mele, A.T.C. Johnson, J.M. Kikkawa, Appl. Phys. Lett. 94 (2009) 111909.
[44] G. Eda, G.Y.Y. Lin, C. Mattevi, H. Yamaguchi, H.A. Chen, I.-S. Chen, C.W. Chen, M. Chhowalla, Adv. Mater. 22 (2009) 505.
[45] S. Kim, Y.T. Lim, E.G. Soltesz, A.M. De Grand, J. Lee, A. Nakayama, J.A. Parker, T. Mihaljevic, R.G. Laurence, D.M. Dor, Nat. Biotechnol. 22 (2004) 93.
[46] R. Weissleder, V. Ntziachristos, Nat. Med. 9 (2003) 123.
[47] P. Cherukuri, C.J. Gannon, T.K. Leeuw, H.K. Schmidt, R.E. Smalley, S.A. Curley, R.B. Weisman, Proc. Natl. Acad. Sci. USA 103 (2006) 18882.
[48] J.H. Choi, M.S. Strano, Appl. Phys. Lett. 90 (2007) 223114.
[49] E.S. Jeng, A.E. Moll, A.C. Roy, J.B. Gastala, M.S. Strano, Nano Lett. 6 (2006) 371.
[50] P.W. Barone, S. Baik, D.A. Heller, M.S. Strano, Nat. Mater. 4 (2005) 86.
[51] J. Chen, H.Y. Liu, W.A. Weimer, M.D. Halls, D.H. Waldeck, G.C. Walker, J. Am. Chem. Soc. 124 (2002) 9034.
[52] T.G. Cha, B.A. Baker, M.D. Sauffer, J. Salgado, D. Jaroch, J.L. Rickus, D.M. Porterfield, J.H. Choi, ACS Nano 5 (2011) 4236.
[53] A. Hartschuh, H. Qian, C. Georgi, M. Boehmler, L. Novotny, Anal. Bioanal. Chem. 394 (2009) 1787.
[54] H.A. Atwater, A. Polman, Nat. Mater. 9 (2010) 205.
[55] P.K. Jain, W. Huang, M.A. El-Sayed, Nano Lett. 7 (2007) 2080.
[56] C.A. Mirkin, Inorg. Chem. 39 (2000) 2258.
[57] S. Nie, S.R. Emory, Science (Washington, DC) 275 (1997) 1102.
[58] K. Kneipp, Y. Wang, H. Kneipp, L.T. Perelman, I. Itzkan, R.R. Dasari, M.S. Feld, Phys. Rev. Lett. 78 (1997) 1667.
[59] K. Aslan, I. Gryczynski, J. Malicka, E. Matveeva, J.R. Lakowicz, C.D. Geddes, Curr. Opin. Biotechnol. 16 (2005) 55.
[60] D. Graham, K. Faulds, D. Thompson, F. McKenzie, R. Stokes, C. Dalton, R. Stevenson, J. Alexander, P. Garside, E. McFarlane, Biochem. Soc. Trans. 37 (2009) 697.
[61] E. Ozbay, Science (Washington, DC) 311 (2006) 189.
[62] J.N. Anker, W.P. Hall, O. Lyanderes, N.C. Shan, J. Zhao, R.P. Van Duyne, Nat. Mater. 7 (2008) 442.
[63] H.-I. Penga, B.L. Miller, Analyst (Cambridge, UK) 136 (2011) 436.
[64] S.K. Ghosh, T. Pal, Chem. Rev. 107 (2007) 4797.
[65] C.C. Huang, Y.F. Huang, Z. Cao, W. Tan, H.T. Chang, Anal. Chem. 77 (2005) 5735.
[66] J. Liu, Y. Lu, Angew. Chem., Int. Ed. Engl. 45 (2006) 90.
[67] J. Liu, Y. Lu, Adv. Mater. 18 (2006) 1667.
[68] H. Li, L. Rothberg, Proc. Natl. Acad. Sci. USA 101 (2004) 14036.
[69] H. Li, L.J. Rothberg, J. Am. Chem. Soc. 126 (2004) 10958.
[70] L. Wang, X. Liu, X. Hu, S. Song, C. Fan, Chem. Commun. (2006) 3780.
[71] C.D. Medley, J.E. Smith, Z. Tang, Y. Wu, S. Bamrungsap, W. Tan, Anal. Chem. 80 (2008) 1067.
[72] G. Liu, X. Mao, J.A. Phillips, H. Xu, W. Tan, L. Zeng, Anal. Chem. 81 (2009) 10013.
[73] F.J. García-Vidal, J.B. Pendry, Phys. Rev. Lett. 77 (1996) 1163.
[74] C.J. Orendorff, L. Gearheart, N.R. Jana, C.J. Murphy, Phys. Chem. Chem. Phys. 8 (2006) 165.
[75] G.V. Maltzahn, A. Centrone, J. Park, R. Ramanathan, M.J. Sailor, T.A. Hatton, S.N. Bhatia, Adv. Mater. 21 (2009) 3175.
[76] J. Jiang, K. Bosnick, M. Maillard, L. Brus, J. Phys. Chem. B 107 (2003) 9964.
[77] S.J. Lee, A.R. Morrill, M. Moskovits, J. Am. Chem. Soc. 128 (2006) 2200.
[78] L. Fabris, M. Dante, G. Braun, S.J. Lee, N.O. Reich, M. Moskovits, T.Q. Nguyen, G.C. Bazan, J. Am. Chem. Soc. 129 (2007) 6086.
[79] G. Braun, S.J. Lee, M. Dante, T.Q. Nguyen, M. Moskovits, N. Reich, J. Am. Chem. Soc. 129 (2007) 6378.
[80] A.J. Bonham, G. Braun, I. Pavel, M. Moskovits, N.O. Reich, J. Am. Chem. Soc. 129 (2007) 14572.
[81] Y. Wang, K. Lee, J. Irudayaraj, Chem. Commun. 46 (2010) 613.
[82] Y.W.C. Cao, R.C. Jin, C.A. Mirkin, Science (Washington, DC) 297 (2002) 1536.
[83] P. Negri, A. Kage, A. Nitsche, D. Naumannc, R.A. Dluhy, Chem. Commun. 47 (2011) 8635.
[84] N.H. Kim, S.J. Lee, M. Moskovits, Nano Lett. 10 (2010) 4181.
[85] H.C. Cheung, in: J.R. Lakowicz (Editor), Topics in Fluorescence Spectroscopy, Plenum, New York, USA, 1991.
[86] T. Zal, R.J. Gascoigne, Curr. Opin. Immunol. 16 (2004) 418.
[87] E.A. Jares-Erijman, T.M. Jovin, Nat. Biotechnol. 21 (2003) 1387.
[88] R.B. Bachilo, M.S. Strano, C. Kittrell, R.H. Hauge, R.E. Smalley, R.B. Weisman, Science (Washington, DC) 298 (2002) 2361.
[89] E.J. Cho, L. Yang, M. Levy, A.D. Ellington, J. Am. Chem. Soc. 127 (2005) 2022.
[90] R.H. Yang, Z.W. Tang, J.L. Yan, H.Z. Kang, Y. Kim, Z. Zhu, W. Tan, Anal. Chem. 80 (2008) 7408.
[91] Z. Zhu, Z. Tang, J.A. Phillips, R. Yang, H. Wang, W. Tan, J. Am. Chem. Soc. 130 (2008) 10856.
[92] E. Treossi, M. Melucci, A. Liscio, M. Gazzano, P. Samorì, V. Palermo, J. Am. Chem. Soc. 131 (2009) 15576.
[93] J. Kim, L.J. Cote, F. Kim, J. Huang, J. Am. Chem. Soc. 132 (2010) 260.
[94] Z. Liu, Q. Liu, Y. Huang, Y. Ma, S. Yin, X. Zhang, W. Sun, Y. Chen, Adv. Mater. 20 (2008) 3924.
[95] Y. Wang, D. Kurunthu, G.W. Scott, C.J. Bardeen, J. Phys. Chem. C 114 (2010) 4153.
[96] H. Dong, W. Gao, F. Yan, H. Ji, H. Ju, Anal. Chem. 82 (2010) 5511.
[97] C.H. Lu, H.H. Yang, C.L. Zhu, X. Chen, G.N. Chen, Angew. Chem., Int. Ed. Engl. 48 (2009) 4785.
[98] S. He, B. Song, D. Li, C. Zhu, W. Qi, Y. Wen, L. Wang, S. Song, H. Fang, C. Fan, Adv. Funct. Mater. 20 (2010) 453.
[99] Y. Wang, Z. Li, D. Hu, C.T. Lin, J. Li, Y. Lin, J. Am. Chem. Soc. 132 (2010) 9274.
[100] C. Fan, S. Wang, J.W. Hong, G.C. Bazan, K.W. Plaxco, A.J. Heeger, Proc. Natl. Acad. Sci. USA 100 (2003) 6297.
[101] C. Huang, S. Chiu, Y. Huang, H. Chang, Anal. Chem. 79 (2007) 4798.
[102] C.C. Huang, C.K. Chiang, Z.H. Lin, K.H. Lee, H.T. Chang, Anal. Chem. 80 (2008) 1497.
[103] D. Zheng, D.S. Seferos, D.A. Giljohann, P.C. Patel, C.A. Mirkin, Nano Lett. 9 (2009) 3258.
[104] T. Förster, Discuss. Faraday Soc. 27 (1959) 7.
[105] R.R. Chance, A. Prock, R. Silbey, Adv. Chem. Phys. 37 (1978) 1.
[106] J.R. Lakowicz, Principles of Fluorescence Spectroscopy, 2nd Edition., Kluwer Academic, New York, USA, 1999.
[107] A.P. Alivisatos, D.H. Waldeck, C.B.J. Harris, Chem. Phys. 82 (1985) 541.
[108] K. Kuhnke, R. Becker, M. Epple, K. Kern, Phys. Rev. Lett. 79 (1997) 3246.
[109] Y. Chen, M.B. O'Donoghue, Y.-F. Huang, H. Kang, J.A. Phillips, X. Chen, M.-C. Estévez, C.J. Yang, W. Tan, J. Am. Chem. Soc. 132 (2010) 16559.
[110] X. Lou, J. Qian, Y. Xiao, L. Viel, A.E. Gerdon, E.T. Lagally, P. Atzberger, T.M. Tarasow, A.J. Heeger, H.T. Soh, Proc. Natl. Acad. Sci. USA 106 (2009) 2989.

Please cite this article in press as: Q. Yuan et al., Trends Anal. Chem. (2012), http://dx.doi.org/10.1016/j.trac.2012.05.010

[111] S.M. Park, J.Y. Ahn, M. Jo, D.K. Lee, J.T. Lis, H.G. Craighead, S. Kim, Lab. Chip 9 (2009) 1206.
[112] M. Haase, H. Schäfer, Angew. Chem., Int. Ed. Engl. 50 (2011) 5808.
[113] F. Wang, D. Banerjee, Y. Liu, X. Chen, X. Liu, Analyst (Cambridge UK) 135 (2010) 1839.
[114] Y. Wang, L. Bao, Z. Liu, D.W. Pang, Anal. Chem. 83 (2011) 8130.
[115] T. Xie, Q. Liu, W. Cai, Z. Chen, Y. Li, Chem. Commun. (2009) 3190.
[116] S.H. Cao, T.T. Xie, W.P. Cai, Q. Liu, Y.Q. Li, J. Am. Chem. Soc. 133 (2011) 1787.
[117] H. Quan, Z. Guo, J. Quant. Spectrosc. Rad. Transfer 93 (2005) 231.
[118] H.Y. Zhu, J.D. Suter, I.M. White, X.D. Fan, Sensors 6 (2006) 785.
[119] C.J. Choi, B.T. Cunningham, Lab. Chip 7 (2007) 550.
[120] S.F. Lin, T.J. Ding, J.T. Liu, C.C. Lee, T.H. Yang, W.Y. Chen, J.Y. Chang, Sensors 11 (2011) 8953.

Please cite this article in press as: Q. Yuan et al., Trends Anal. Chem. (2012), http://dx.doi.org/10.1016/j.trac.2012.05.010